Apoptosis (2024) 29:321–330
https://doi.org/10.1007/s10495-023-01899-1

Different bacterial cargo in apoptotic cells drive distinct macrophage phenotypes

Ana Carolina Guerta Salina[1,2,3] · Letícia de Aquino Penteado[1,2] · Naiara Naiana Dejani[4] · Ludmilla Silva-Pereira[1] · Breno Vilas Boas Raimundo[1] · Gabriel Ferranti Corrêa[1] · Karen Cristina Oliveira[1] · Leandra Naira Zambelli Ramalho[6] · Mèdéton Mahoussi Michaël Boko[5] · Vânia L. D. Bonato[2,5] · C. Henrique Serezani[3] · Alexandra Ivo Medeiros[1]

Accepted: 22 September 2023 / Published online: 5 October 2023

Abstract

The removal of dead cells (efferocytosis) contributes to the resolution of the infection and preservation of the tissue. Depending on the environment milieu, macrophages may show inflammatory (M1) or anti-inflammatory (M2) phenotypes. Inflammatory leukocytes are recruited during infection, followed by the accumulation of infected and non-infected apoptotic cells (AC). Efferocytosis of non-infected AC promotes TGF-β, IL-10, and PGE_2 production and the polarization of anti-inflammatory macrophages. These M2 macrophages acquire an efficient ability to remove apoptotic cells that are involved in tissue repair and resolution of inflammation. On the other hand, the impact of efferocytosis of infected apoptotic cells on macrophage activation profile remains unknown. Here, we are showing that the efferocytosis of gram-positive *Streptococcus pneumoniae*-AC (*Sp*-AC) or gram-negative *Klebsiella pneumoniae*-AC (*Kp*-AC) promotes distinct gene expression and cytokine signature in macrophages. Whereas the efferocytosis of *Kp*-AC triggered a predominant M1 phenotype in vitro and in vivo, the efferocytosis of *Sp*-AC promoted a mixed M1/M2 activation in vitro and in vivo in a model of allergic asthma. Together, these findings suggest that the nature of the pathogen and antigen load into AC may have different impacts on inducing macrophage polarization.

Keywords Macrophages · Efferocytosis · Infected apoptotic cells · Lung inflammation

Ana Carolina Guerta Salina and Letícia de Aquino Penteado have contributed equally to this work.

✉ Alexandra Ivo Medeiros
alexandra.medeiros@unesp.br

[1] Department of Biological Sciences, School of Pharmaceutical Sciences, São Paulo State University (UNESP), Araraquara, São Paulo, Brazil

[2] Basic and Applied Immunology Program, Ribeirao Preto Medical School, University of São Paulo (USP), Ribeirão Preto, São Paulo, Brazil

[3] Division of Infectious Diseases, Department of Medicine, Vanderbilt University Medical Center (VUMC), Nashville, TN, USA

[4] Department of Physiology and Pathology, Federal University of Paraíba (UFPB), João Pessoa, Paraíba, Brazil

[5] Department of Biochemistry and Immunology, Ribeirao Preto Medical School, University of São Paulo (USP), Ribeirão Preto, São Paulo, Brazil

[6] Department of Pathology and Legal Medicine, Ribeirao Preto Medical School, University of São Paulo (USP), Ribeirão Preto, São Paulo, Brazil

Introduction

Apoptotic cell (AC) clearance, termed efferocytosis, is a multi-step process crucial to maintaining physiological tissue integrity and restoring tissue homeostasis after microbial infection or chronic inflammatory disorder [1]. Cell death is a common consequence of infections, and efferocytosis of dying infected cells can either contribute to prevent the spread of infections or benefit the pathogen dissemination using Trojan-horse-type mechanisms [2]. We and others have demonstrated that recognizing *Escherichia coli*–infected apoptotic neutrophils by bone marrow–derived dendritic cells (BMDCs) leads to a cytokine milieu that favors Th17 cell differentiation [3, 4]. Conversely, BMDC-mediated efferocytosis of *Streptococcus pneumoniae*–infected apoptotic cells (*Sp*-AC) induces the differentiation and expansion of Th1 lymphocytes [5]. Whereas TLR4 and MyD88 molecules are necessary for recognizing of gram-negative bacteria inside the AC [6, 7], the response of BMDC towards *S.*

pneumoniae, a gram-positive bacterium, depends on bacteria recognition by the adaptor protein RIP2 [5].

Macrophages are immune cells that originate from embryonic progenitors or recruited monocytes. Tissue-resident macrophages compose a diverse population strategically distributed throughout every organ and are amongst the first cells to respond to infection [8]. These cells are highly plastic and equipped with a vast repertoire of pattern recognition and cytokine/chemokine receptors that enable macrophages to respond to environmental cues and acquire an inflammatory or pro-resolution phenotype [9]. The pro-inflammatory phenotype of macrophages is characterized by high production of reactive nitrogen and oxygen species and pro-inflammatory cytokines. Therefore, these cells participate in the acute response to infection and tissue injury. In contrast, the pro-resolving programming in macrophages mediates tissue repair and the re-establishment of homeostasis. These cells have robust production of TGF-β and IL-10 and are an abundant source of polyamines. The clearance of AC is often associated with acquiring a pro-resolution phenotype of macrophages, and those macrophages acquire a higher ability to phagocyte AC than the pro-inflammatory macrophages. However, the effect of recognition of AC infected with gram-positive or gram-negative bacteria on the phenotype acquired by macrophages remains elusive.

Asthma is a chronic inflammatory disease that affects approximately 339 million people worldwide. The hallmark of allergic asthma, which affects approximately 50% of asthmatic people, is the eosinophil recruitment in the bronchoalveolar fluid (BALF) induced by Th2 $CD4^+$ T cells that secrete IL-4, IL-5, and IL-13. This immune response leads to excessive mucus production, bronchial airway hyperresponsiveness (AHR), tissue damage, and remodeling [10]. Th2-dominant microenvironment with high levels of IL-4 and IL-13 favors the predominance of the M2 macrophages. Asthma is, however, a heterogeneous disease. In non-allergic asthma, neutrophil accumulation in the airways releases proteases and extracellular DNA traps that can contribute to tissue damage [11]. Asthma severity was associated with the increased neutrophil burden [12], and patients with neutrophilic asthma are resistant to inhaled corticosteroids, the gold standard treatment for asthma [13]. It has been reported that asthmatic patients have a higher risk of developing pneumonia following infection with *S. pneumoniae* [14]; however, whether efferocytosis of infected cells by resident macrophages during asthma could play a role in changing the microenvironment of eosinophilic asthma by shifting the pro-resolving program of macrophage to an inflammatory phenotype is unknown.

Here, we investigated whether pathogen-associated molecular patterns (PAMPs) derived from *Streptococcus pneumoniae* or *Klebsiella pneumoniae* during the efferocytosis of infected apoptotic cells might impact macrophage polarization. We observed that efferocytosis of *S. pneumoniae*-infected apoptotic cells (*Sp*-AC) promoted a mixed M1/M2 profile. In contrast, efferocytosis of *K. pneumoniae*-infected apoptotic cells (*Kp*-AC) triggered a predominant M1 phenotype that was partially dependent on toll-like receptor-4 (TLR4) signaling. Instillation of *Kp*-AC led to proinflammatory cytokine production in the lungs of mice as well as a tendency towards the M1 phenotype of lung macrophages. In a model of OVA-induced allergic asthma, instillation of *Sp*-AC increased IL-12 levels and reduced M2 markers expression, suggesting that efferocytosis of *Sp*-AC might shift macrophage response in allergic asthma to produce a cytokine milieu that could antagonize type 2 responses during asthma.

Results

Efferocytosis of *S. pneumoniae* or *K. pneumoniae*-infected apoptotic cells impacts macrophage polarization in vitro

Streptococcus pneumoniae and *Klebsiella pneumoniae* infection induces intense recruitment of neutrophils that play an essential role during bacteria clearance, and these infected neutrophils become an important source of AC. We and other groups have shown that the efferocytosis of infected apoptotic cells, such as *E. coli* and *S. pneumoniae*, by dendritic cells, promotes distinguished $CD4^+$ T cell subset differentiation [4, 5].

Similarly to dendritic cells, macrophages also play a crucial role in the clearance of infected-AC during infection. Given that the cargo inside the apoptotic cell alters dendritic cell properties that affect the $CD4^+$ T cell differentiation, we hypothesized that the pathogen-associated molecular patterns (PAMPs) derived from *S. pneumoniae* or *K. pneumoniae* during the efferocytosis of infected AC might also impact macrophage polarization. HL-60 neutrophil-like cells were incubated in the presence of *S. pneumoniae* or *K. pneumoniae* previously stained with CFSE for 2 h. We observed that around 70–90% of cells were CFSE-labeled, indicating *S. pneumoniae* or *K. pneumoniae* phagocytosis by HL-60 cells (Supplemental Data Fig. 1a and b). The infected neutrophils were then submitted to UV-irradiation (1 mJ) to induce apoptosis (Supplemental Data Fig. 1c). BMDMs were incubated for 2 h with non-infected-AC, *Sp*-AC, or *Kp*-AC stained with CFSE to assess macrophage efferocytosis. After 2 h of incubation, we found that more than 90% of BMDM were AC-$CFSE^+$ macrophages (Supplemental Data Fig. 1d and e). To determine whether efferocytosis of *Sp*-AC or *Kp*-AC could impact macrophage polarization, BMDMs were incubated with AC, *Sp*-AC, or *Kp*-AC for 2 h and then washed to remove the non-engulfed ACs, and

these cells were incubated for another 24 h to evaluate M1 and M2 macrophage markers. Interestingly, we found that the efferocytosis of *Sp*-AC induced a slight increase of both M1 and M2 markers, such as *Ccr7* and *Fizz1* (Fig. 1b, d), as well as a significant increase of NO and IL-1β production by BMDM compared to M0 and M0 + AC (Fig. 1f, h). In contrast, phagocytosis of *Kp*-AC led to a slight increase of *Ccr7* and a minor decrease of *Arg1* and *Cd206*, as well as higher levels of nitrite, TNF-α, and IL-1β compared to M0, while no significant differences of IL-10 levels were detected when comparing the different conditions with AC (Fig. 1b, c, e, f, g, h, i). Thus, the presence of *S. pneumoniae* inside the AC resulted in a mixed BMDM phenotype compared to *Kp*-AC recognition, which led to a prominent M1 phenotype.

Efferocytosis of *Kp*-AC drives an M1 macrophage phenotype partially through TLR4-mediated signaling pathway

Previous studies have shown that the efferocytosis of *E. coli* or *C. rodentium*-infected apoptotic cells by BMDC induces IL-6, IL-1β, and TGF-β production through TLR4 [6, 7]. Given that *K. pneumonia*-derived lipopolysaccharide is a potential ligand for TLR4, we evaluated whether the expression of M1 markers in BMDM and the higher levels of inflammatory mediators during the efferocytosis of *Kp*-AC may be partly due to TLR4 activation. BMDMs from WT and TLR4 K.O. mice were incubated for 2 h with *Kp*-AC, then washed to remove the non-engulfed ACs, and M1 and M2 markers and cytokine production were evaluated. The deficiency of TLR4 in BMDMs showed a modest decrease in the expression of M1 markers, such as *Ccr7*, and led to a discrete increase in the expression of M2 markers, such as *Arg1* and *Cd206*, compared to BMDMs from WT animals (Fig. 2b, c, e). Furthermore, the absence of TLR4 modestly inhibited the production of TNF-α and IL-10, and significantly reduced the production of IL-1β compared to BMDMs from WT animals (Fig. 2g–i). These results suggest that, as previously observed in BMDC, *K. pneumonia*-derived lipopolysaccharide recognition via TLR4 seems to be a contributing signaling pathway involved in macrophage polarization during *Kp*-AC efferocytosis.

Infected *Kp*-AC drives a pro-inflammatory phenotype of macrophages in the lung

Previous studies have shown that the instillation of non-infected apoptotic cells before the *K. pneumoniae*-infection

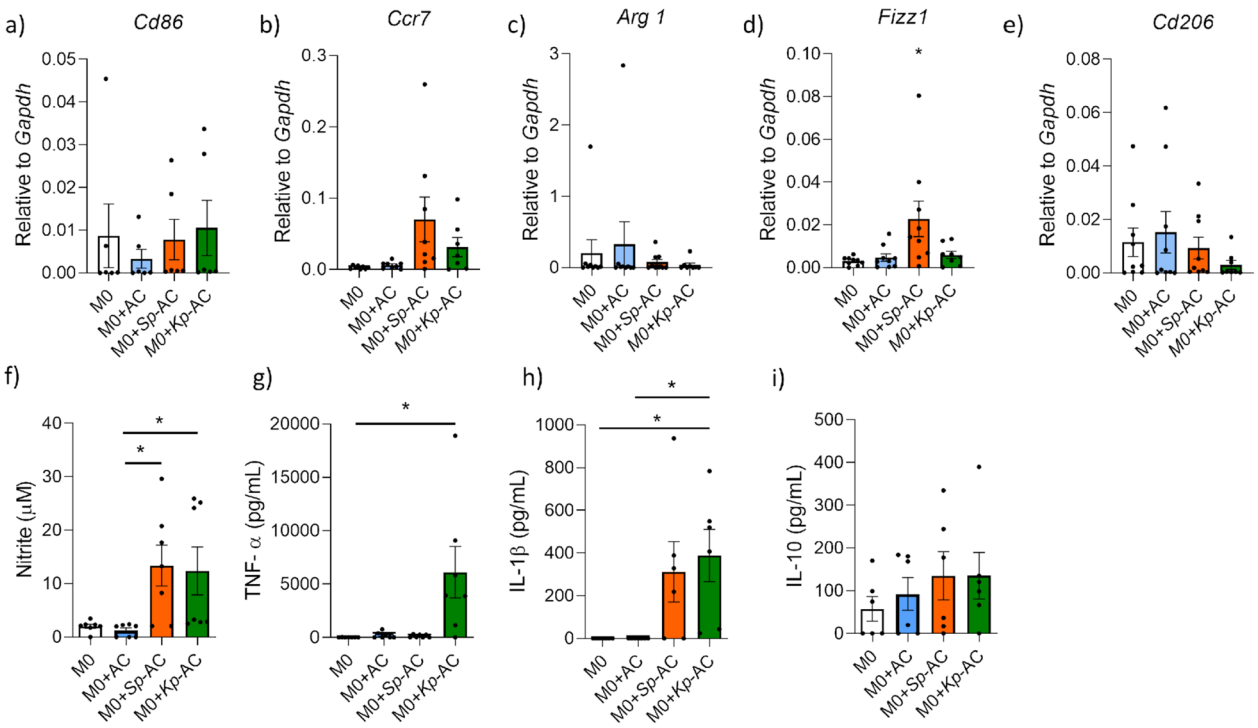

Fig. 1 Different sources of apoptotic cells phagocytosis modulate macrophage phenotype in vitro. BMDMs were co-cultured with AC, *Sp*-AC, and *Kp*-AC at a 1:3 ratio for 2 h. Non-engulfed cells were removed, and macrophages were incubated for another 24 h. Cells were lysed for RNA extraction and RT-qPCR analysis for the gene expression of **a** *Cd86*, **b** *Ccr7*, **c** *Arg1*, **d** *Fizz1*, and **e** *Cd206*. Supernatant was collected to quantify **f** nitrite, **g** TNF-α, **h** IL-1β, and **i** IL-10 by ELISA. Data represent mean ± SEM of at least seven independent experiments. *P < 0.05 compared with M0, M0 + AC, M0 + *Sp*-AC, M0 + *Kp*-AC

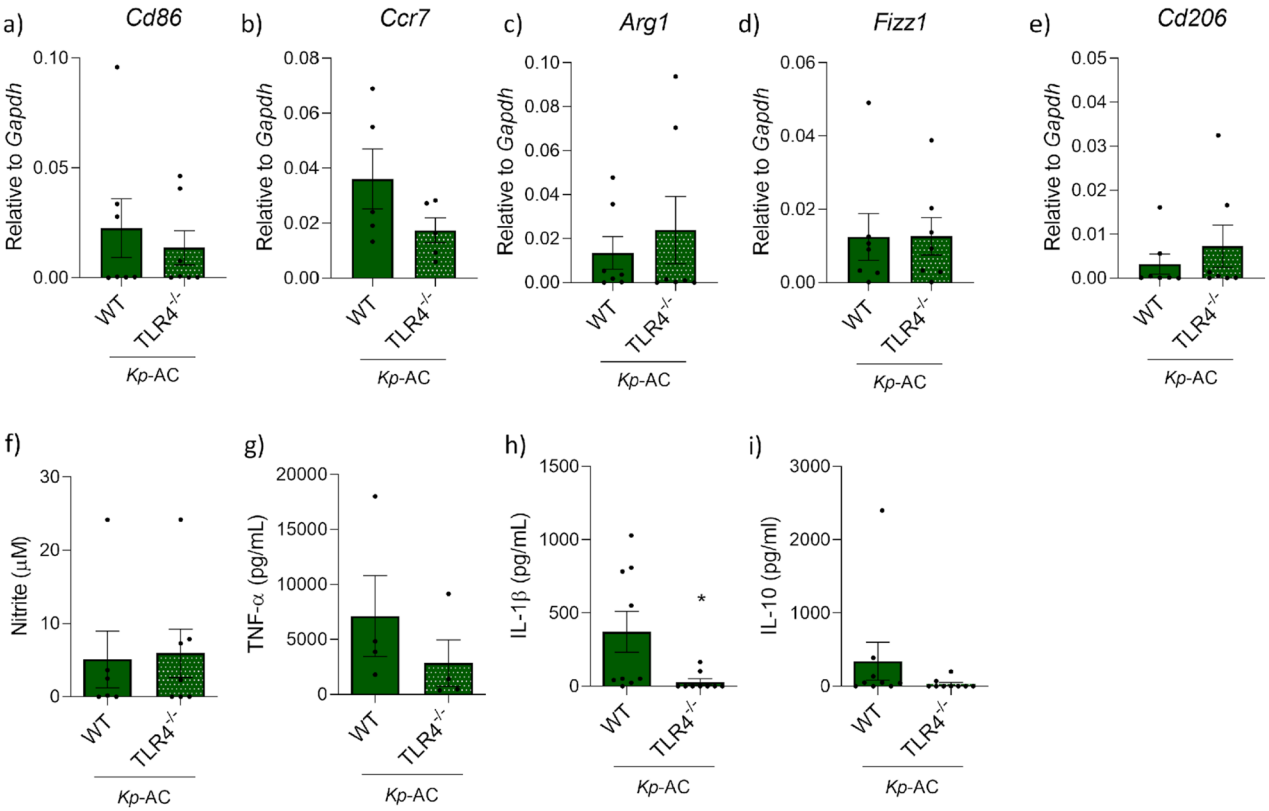

Fig. 2 *Kp*-AC triggers TLR4 engagement on BMDM and to promote M1 polarization in vitro. BMDMs from WT or TLR4 K.O. mice were co-cultured with *Kp*-AC at a 1:3 ratio for 2 h. Non-engulfed cells were removed, and macrophages were incubated for another 24 h. Cells were lysed for RNA extraction and RT-qPCR analysis for the gene expression of **a** *Cd86*, **b** *Ccr7*, **c** *Arg1*, **d** *Fizz1*, **e** *Cd206*, and the supernatant was collected for the quantification of **f** nitrite, **g** TNF-α, **h** IL-1β, and **i** IL-10 by ELISA. Data represent the mean ± SEM of four independent experiments. *P < 0.05 compared with WT

increases CFU and promotes bacteremia [15]. Given that *Sp*-AC efferocytosis by M0 had a modest impact on M1/M2 expression markers and inflammatory cytokine production, we sought to evaluate whether the efferocytosis of *Kp*-AC could also activate alveolar and lung macrophages and promote polarization to pro-inflammatory macrophages in a similar manner observed for BMDM. For this purpose, the animals were instilled with 10^7*Kp*-AC, and, 24 h later, macrophages were isolated from lungs using F4/80-magnetic beads. As we observed in vitro, the lung macrophages isolated from mice receiving *Kp*-AC expressed higher pro-inflammatory markers, such as *Cd86* and *Nos2*, and lower *Cd206* than PBS-treated control mice (Fig. 3a). Also, lung homogenate from *Kp*-AC mice had high levels of inflammatory cytokines, such as IL-β, IL-6, TNF-α, and a slight increase of IL-12 (Fig. 3b). Alveolar macrophages obtained in the bronchoalveolar lavage from mice instilled with *Kp*-AC expressed slightly higher levels of *Cd86* and lower *Cd206* and *Ymz1* gene expression (Fig. 3c). We also detected increased IL-1β, IL-6, TNF-α, and IL-10 production in the bronchoalveolar lavage fluid (BALF) compared to PBS-treated control mice (Fig. 3d). These results suggest that the efferocytosis of *Kp*-AC during the infection drives pro-inflammatory macrophage polarization and directly or indirectly impacts the lung microenvironment.

Impact of AC or *Sp*-AC in lung inflammation in OVA-induced murine allergic asthma

Asthma severity is associated with M2 macrophages known to have a higher ability to remove AC. Apoptosis of eosinophils decreases allergic lung inflammation in mice [16]; however, it is still unknown whether this attenuation of inflammation could be related to the clearance of apoptotic eosinophils by macrophages. We next investigate whether efferocytosis in an OVA-induced murine allergic asthma model could alter the pulmonary microenvironment of Th2 cytokines responsible for maintaining the M2 profile of macrophages. For that, WT mice were sensitized and challenged with OVA, and after 3 days, the mice were instilled with non-infected AC (AC) or *S. pneumoniae*-infected apoptotic cells (*Sp*-AC). After 24 h, the expression of M1 and M2 markers and the production of cytokines were evaluated in the cells and supernatants of BALF, respectively. Lung histology confirmed asthma

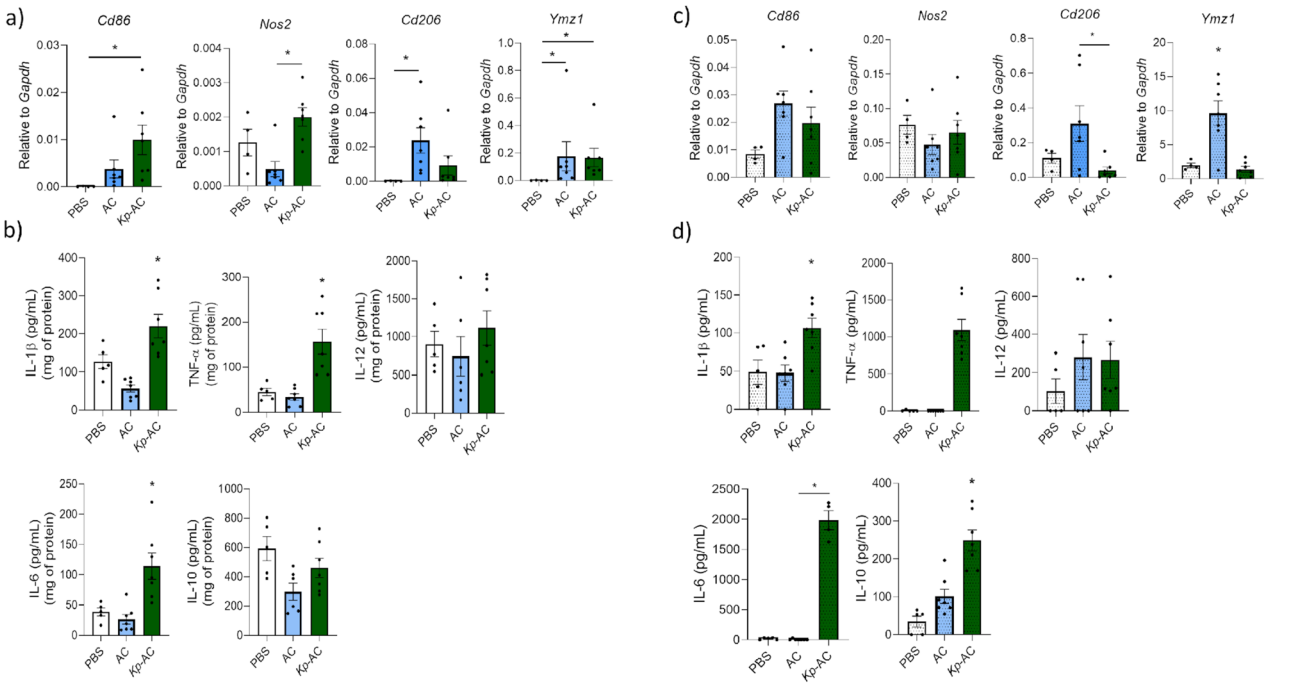

Fig. 3 Efferocytosis of *Kp*-AC in the lungs drives inflammation. C57BL/6 mice were inoculated with 10^7*Kp*-AC in 30 µL of PBS (i.n.) (n = 7 mice/group). Control mice were inoculated with PBS alone by the same route (n = 5 mice/group). 24 h later, the animals were euthanized, lungs were digested with collagenase D, and macrophages were isolated for RT-qPCR analysis (**a**) and cytokine quantification (**b**). Cells in the bronchoalveolar lavage fluid (BALF) were collected for gene expression analysis by RT-qPCR (**c**), and cytokine quantification was performed in BALF by ELISA (**d**). Data were pooled from two independent experiments and are mean ± SEM. *P < 0.05 compared with PBS and AC

induction, which showed a discrete peribronchial inflammation in the PBS-OVA group, while AC and *Sp*-AC exhibited similar lung inflammation (Supplemental Data Fig. 2). As expected, BALF cells from OVA-sensitized and challenged mice increased the M2 markers compared to non-sensitized and non-challenged mice (PBS group). The presence of *S. pneumoniae* inside the apoptotic cell (*Sp*-AC group) reduced the expression of *Arg1*, *Cd206*, and *Ymz1* and increased the expression of *Fizz1* and *Nos2* compared to the group receiving AC (Fig. 4a–f). In the BALF, AC instillation resulted in the inhibition of IL-1β and IL-12 compared to the BALF of PBS-OVA animals, whereas the presence of the bacteria inside the AC led to an increase in IL-12 and IL-10 levels compared to the group AC (Fig. 4h, i, k). These findings show that *Sp*-AC in a microenvironment of type 2 inflammation induces a mixed M1/M2 pattern of macrophages and cytokines that may negatively modulate the lung inflammation in asthmatic mice.

Discussion

Microenvironment milieu, pathogens and apoptotic cells influence macrophage polarization and function [1, 2]. In the early stages of infection, PRR-mediated recognition of Gram-positive or Gram-negative bacteria triggers inflammation and expression of M1 or M2 markers [17–19]. Also, cell death is frequent in the infection process, and the clearance of AC may affect the macrophage activation profile. Recognition of non-infected apoptotic cells favors macrophage secretion of IL-10, TGF-β, and PGE_2, leading to a pro-resolving phenotype [20]. However, the impact of efferocytosis of infected apoptotic cells on macrophage activation profile remains elusive. Here, we determined the expression of M1 and M2 markers and cytokine production during efferocytosis of *S. pneumoniae* or *K. pneumoniae*-infected HL-60 neutrophil-like cells. We showed that the efferocytosis of *Kp*-AC and *Sp*-AC promoted distinct gene expression and cytokine signature in macrophages. Efferocytosis of *Sp*-AC promoted a mixed expression of M1/M2 markers, *Ccr7*, and *Fizz1* and induced IL-1β and NO production in vitro. In contrast, efferocytosis of *Kp*-AC triggered a predominant M1 phenotype, partially through TLR4 pathway, with higher *Ccr7*, lower *Fizz1*, and *Cd206* expression and enhanced TNF-α, IL-1β, and NO production by BMDM.

During an infection, neutrophils are recruited to the affected tissue to clear pathogens. Host and pathogen products affect neutrophils' lifespan, causing neutrophil apoptosis [21, 22]. In this regard, we previously demonstrated that efferocytosis of *E. coli*-infected cells enhances dendritic cell maturation [3] and the generation of cytokines that trigger

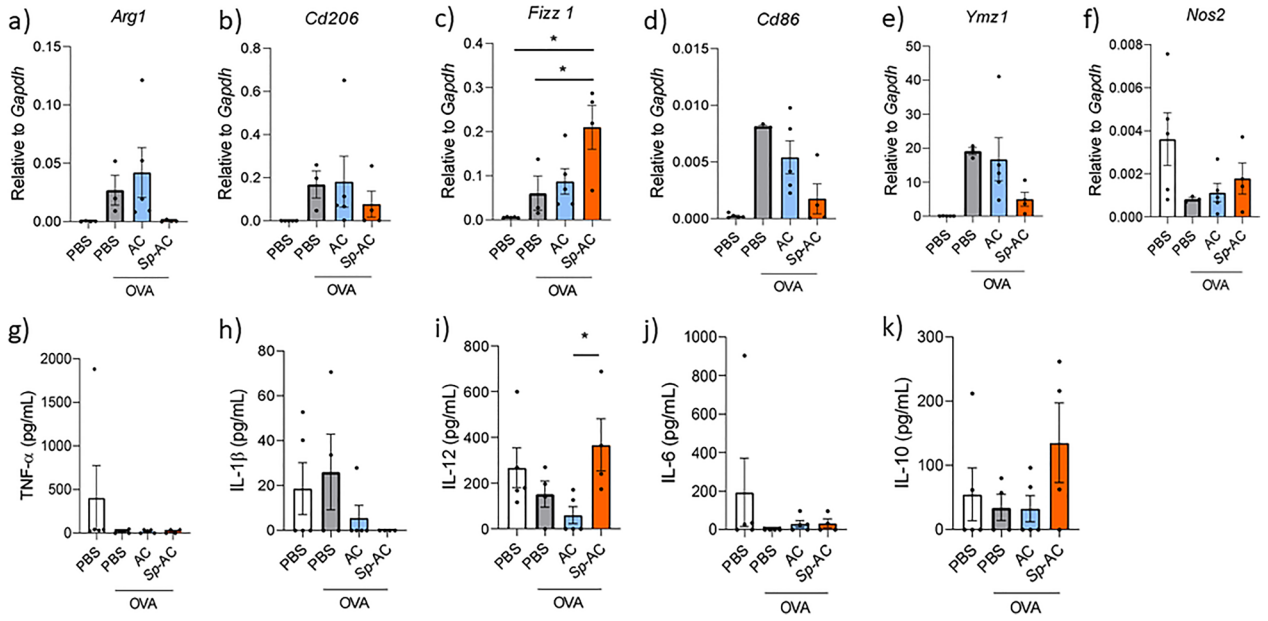

Fig. 4 Efferocytosis of *Sp*-AC affects macrophage phenotype and cytokine microenvironment in the lung of asthmatic mice. C57BL/6 mice were sensitized 3 times with 10 µg of ovalbumin (OVA) Grade-VI emulsified in 2 mg of aluminum hydroxide by intraperitoneal route with 7-day intervals between injections. Animals were challenged intranasally for 3 consecutive days with 30 µg of OVA Grade V 7 days after the third sensitization. Mice were intranasally inoculated with 10^7*Sp*-AC or AC in 30 µL of PBS. Control mice were inoculated with PBS alone by the same route. 24 h later, the animals were euthanized, and bronchoalveolar lavage fluid (BALF) was collected. Cells in the BALF were collected for RT-qPCR analysis of the gene expression of **a** *Arg1*, **b** *Cd206*, **c** *Fizz1*, **d** *Cd86*, **e** *Ymz1*, and **f** *Nos2*, and cytokine quantification of **g** TNF-α, **h** IL-1β, **i** Il-12, **j** IL-6, and **k** IL-10 was performed on BALF by ELISA. Data were pooled from two independent experiments and are mean ± SEM. *P < 0.05 compared with PBS and AC

Th17 cell differentiation [4]. In contrast, efferocytosis of *S. pneumoniae*-infected cells creates a microenvironment that favors Th1 expansion [5]. As observed in BMDC activation, macrophages also polarized into different subsets in the presence of *Kp*-AC or *Sp*-AC, suggesting that AC-carrying other bacterial products modulate macrophage activation. Although previous studies have shown that *S. pneumoniae* infection can trigger an intense inflammatory response with predominant polarization of macrophages to an M1 pattern by the recognition of lipoteichoic acid, a membrane bacterial component, and pneumolysin toxin via TLR2 and TLR4, respectively [23], Goldman et al. have shown that peritoneal macrophages infected with *S. pyogenes* resulted in mixed M1/M2 polarized macrophages, consistent with our results [24]. Furthermore, *S. pneumoniae* components may have a potential strategy to suppress macrophage polarization toward an M1 profile. Also, during *Sp*-AC efferocytosis, ligands from the apoptotic body that induce a non-inflammatory signal may inhibit the activation in response to TLR ligands from *S. pneumoniae*, and our findings demonstrated that TLR ligands from *S. pneumoniae* seem less potent than LPS in driving macrophage polarization.

Considering that *Kp*-AC triggered proinflammatory macrophage activation, we evaluated whether TLR4 signaling could be involved in M1 polarization by efferocytosis of *Kp*-AC. An elegant study by Torchinsky et al. demonstrated that efferocytosis of LPS-blasts by TLR4$^{-/-}$ or MyD88$^{-/-}$Trif$^{-/-}$ BMDCs did not induce Th17 cell differentiation as observed for BMDC from WT mice [7]. The lack of TLR4 in macrophages during the efferocytosis of *Kp*-AC partially inhibited M1 polarization but, instead, drove M2 phenotype. The absence of TLR4 signaling showed significant inhibition of IL-1β production, a modest inhibition of TNF-α, and IL-10, as well as *Ccr7*, *Arg1*, and *Cd206* expression, compared to BMDM from WT animals. Thus, TLR4-ligands from *K. pneumoniae* can drive M1-polarized macrophages during the efferocytosis of *Kp*-AC. Interestingly, although previous studies have shown that efferocytosis of non-infected cells induce M2 phenotype and IL-10 production by alveolar and peritoneal macrophages [25, 26], efferocytosis of non-infected HL-60 apoptotic cells did not alter *Arg1*, *Fizz1*, and *Cd206* mRNA expression, as well as IL-10 production by BMDM. This finding suggests that the source of apoptotic cells and the type of macrophage might be important factors driving the M2 phenotype during efferocytosis.

Efferocytosis in pulmonary tissue controls inflammation and maintains lung homeostasis [27]. Previous reports have shown that apoptotic cell instillation improves pulmonary inflammation resolution in LPS-stimulated lungs [28].

Non-infected AC or *Kp*-AC was instilled in mice to evaluate the impact of recognizing different sources of apoptotic cells in lung inflammation and macrophage polarization. Consistent with previous findings, the instillation of non-infected-AC in vivo led to a modest increase in the expression of M2 markers, *Cd206* and *Ymz1*. On the other hand, the instillation of *Kp*-AC caused prominent pro-inflammatory cytokine production in the lungs of mice, as well as a trend towards increasing M1 markers mainly in F4/80 cells from lung homogenate, confirming the in vitro results. Indeed, efferocytosis of *Kp*-AC decreased the expression of the M2 marker *Cd206* and enhanced iNOS abundance and IL-6 production, similar to Li et al. findings in mice infected with *K. pneumoniae* [18].

Allergic asthma is a chronic inflammatory disease characterized by eosinophilic airway inflammation, type 2 cytokines, and enhanced levels of IgE specific to allergens [29]. However, the heterogeneity of asthma also includes a non-allergic form of the disease, in which neutrophilic or granulocytic inflammation prevails in the lung [30]. While M1 is related to neutrophil infiltration, M2 response in asthma involves eosinophil recruitment into the lungs [31]. Patients with asthma have an increased risk of pulmonary infections, such as invasive pneumococcal disease [30, 32]. *S. pneumoniae* infection may attenuate allergic lung inflammation by damping the Th2 response [33] or even driving severe asthma by promoting Th17 responses, neutrophil infiltration, lung inflammation, and airway hyperresponsiveness [34]. Consistent with our findings, the instillation of *Sp*-AC increased IL-12 and IL-10 levels and reduced M2 markers expression, suggesting that efferocytosis of *S. pneumoniae*-infected cells modulates macrophage response in allergic asthma and produces a cytokine milieu that may antagonize Th2 inflammation. The presence of *S. pneumoniae* inside of apoptotic cells might be a determinant factor to increase IL-12 production, a Th1-inducing cytokine, and decrease M2 markers during efferocytosis, while IL-10 induced by efferocytosis of *Sp*-AC may be essential to limit lung inflammation. Indeed, the lungs of animals exposed to the allergen followed by instillation *Sp*-AC showed a reduction of pulmonary inflammation, suggesting that IL-10 could negatively modulate allergic asthma.

In summary, our data suggest that the bacterial cargo in AC affects macrophage activation during efferocytosis. Recognition of *K.* pneumoniae-infected cells induced a pro-inflammatory response in vitro and in vivo, whereas *S. pneumoniae*-infected cells promoted mixed expression of activation markers by macrophages and a cytokine milieu that may modulate inflammation in the lung of mice exposed to the allergen. We focused on investigating the production of cytokines and macrophage markers in a short time after AC instillation. Thus, further studies are necessary to determine whether late effects of efferocytosis of *S. pneumoniae* infected cells could promote Th1/Treg induction in allergic asthma to dampen Th2 response and the outcome of bacteria recognition in shifting eosinophilic asthma to neutrophilic asthma through macrophage plasticity.

Materials and methods

Animals

C57BL/6 mice were purchased from the Animal Facility of the Multidisciplinary Center for Biological Research (CEMIB/UNICAMP), the Biotério Geral (FMRP/USP), and from the Centro de Pesquisa e Produção de Animais (CPPA/UNESP). Toll-like receptor-4 knockout animals (B6.129-Tlr4^{tm1Kir}/J) were purchased from Biotério Geral (FMRP/USP). The animals were maintained with controlled temperature, humidity, airflow, and dark/light cycle with free access to sterilized water and food. Animals were housed and bred under specific pathogen-free conditions. All animal experiments were carried out under ethical guidelines and approved by the Institutional Animal Care and Committee from the School of Pharmaceutical Sciences, São Paulo State University.

Bacterial strains

Streptococcus pneumoniae strain ATCC 49,619 and *Klebsiella pneumoniae* (clinical isolate) were donated by Prof. Dr. Ana Gales. Both bacteria were maintained at − 80 °C and reactivated by culturing in Tryptic Soy Broth (TSB) at 37 °C with shaking for 6 h for *S. pneumoniae* or overnight for *K. pneumoniae*. After reactivation, subcultures were grown in TSB medium at 37 °C with shaking. To determine the bacterial concentration, *S. pneumoniae* and *K. pneumoniae* were plated in Blood Agar or McConkey Agar, respectively, using serial dilution. The bacteria were maintained at 4 °C and used the next day according to the CFU obtained the day before. When indicated, bacteria were stained with 5 µm of CFSE (Invitrogen) according to manufacturer's protocol.

Generation of infected apoptotic cells

HL-60 cells (BCRJ Code: 0104) were differentiated into neutrophil-like cells with 1.2% DMSO for 72 h. Then, cells were incubated with *S. pneumoniae* or *K. pneumoniae* at a ratio of 1:30 for 2 h to allow phagocytosis and infection. Cells were extensively washed with PBS to remove bacteria and cellular debris. To induce apoptosis, infected cells were exposed to 1 mJ of UV-irradiation in a UV Crosslinker 365 nm and maintained in a humidified 37 °C 5% CO_2 incubator for 4 h. Cell death was confirmed by annexin-V and 7-aminoactinomycin D staining (BD

Biosciences, Mountain View, CA). Cells were acquired on a FACSVerse (BD Biosciences) and data analysis was performed using FlowJo 10 software (Tree Star, San Carlo, CA, USA).

Generation of bone-marrow-derived-macrophages

BMDMs were differentiated from bone marrow precursor cells of 6–8 weeks old C57BL/6 mice. Cells were cultured in 100 × 20-mm tissue culture plates (Falcon; BD Biosciences, Mountain View, CA) with 10 ml of complete DMEM medium (Lonza Walkersville, Rockville, MD) supplemented with sodium pyruvate, non-essential amino acids, 10% of fetal bovine serum, 10 µg/ml gentamicin (Life Technologies, Grand Island, NY), 60 ng/ml of M-CSF, and 20 ng/ml of GM-CSF (PeproTech, Rocky Hill, NJ). 10 ml of supplemented DMEM medium were added on the third and replaced on the 6th day. On the 7th day, non-adherent cells were discarded, and adherent macrophages were collected.

Efferocytosis and macrophage polarization assay

After induction of apoptosis, *Sp*-AC and *Kp*-AC were stained with CFSE (Invitrogen) and cultured with BMDMs for 2 h at a 3:1 AC: macrophage ratio. After 2 h, unbound ACs were removed by vigorous rinsing of the monolayer, and cells were incubated for 24 h in a humidified 37 °C, 5% CO_2 incubator. To determine the efferocytosis rate, *Sp*-AC, and *Kp*-AC were stained with CFSE according to the manufacturer's protocol, and the percentage of efferocytosis by BMDM was determined by Flow Cytometry. Cells were acquired on a FACSVerse (BD Biosciences), and data analysis was performed using FlowJo 10 software (Tree Star, San Carlo, CA, USA).

RNA from BMDM or tissue cells

BMDM or lung macrophage RNA was isolated using RNAspin Mini Kit (GE) according to the manufacturer's instructions (GE Healthcare) and reverse-transcribed into cDNA using the iScript cDNA Synthesis Kit (BioRad). The purity and concentration of the RNA were determined using a spectrophotometer. Gene expression was determined by amplification with specific primers and quantification by SybrGreen (Life Technologies, Grand Island, NY) on a 7500 Real-Time PCR system (Applied Biosystems). The relative gene expression was calculated by the $2^{-\Delta Ct}$ method. Expression of genes of interest was normalized to the expression of the housekeeping gene *Gapdh*. Primer sequences are listed in Supplementary Table 1.

Enzyme-linked immunosorbent assay (ELISA)

The supernatant following efferocytosis in vitro, the tissue homogenate, and BALF were quantified for the presence of IL-6, IL-1β, IL-10, TNF-α, IL-12 (p40/p70), and TGF-β. The minimum detectable concentrations are 62.5 pg/ml for IL-12; 31.25 pg/ml for IL-10 (BD Pharmingen); 15.6 pg/ml for IL-1β, IL-6, TGF-β, and TNF-α (DuoSet ELISA; BD Pharmingen and R&D Systems). All procedures were performed according to the manufacturer's instructions.

Nitrite quantification

Nitric oxide production was assessed by measuring its stable end product, nitrite, by Griess reaction using a mix of an equal volume of sulphanilamide and N-1-napthylethylenediamine dihydrochloride (NEED). Nitrite concentrations were estimated using a standard nitrite curve.

In vivo macrophage polarization

C57BL/6 mice aged 6 to 8-weeks old were anesthetized with xylazine and ketamine and intranasally inoculated with 10^7 *Kp*-AC in 30 µL of PBS. For control, mice were inoculated with PBS alone by the same route. After 24 h, the animals were euthanized, and bronchoalveolar lavage fluid (BALF) was collected by aspiration of ice-cold PBS for cytokine detection. Cells in BALF were counted, lysed, and RNA was extracted for gene expression analysis by RT-qPCR. The lung was collected and divided for cytokine quantification and macrophage isolation. For lung macrophage isolation, the lung was first homogenized with a GentleMACS Dissociator (Miltenyi Biotec), then enzymatically digested with 1.6 mg/ml of collagenase D for 1 h. Single-cell suspensions were stained with anti-CD16/32 before staining with F4/80 antibody conjugated with phycoerythrin (PE). Then, PE + cells were isolated using Anti-PE MicroBeads (Miltenyi Biotec) according to the manufacturer's instructions. Isolated cells were kept in a lysis buffer for gene expression analysis by RT-qPCR.

OVA-induced asthma model

The OVA-induced asthma model was performed as previously described [35]. Briefly, C57BL/6 mice were sensitized 3 times with 10 µg of ovalbumin (OVA) Grade-VI emulsified in 2 mg of aluminum hydroxide (Sigma-Aldrich, St. Louis, MO, USA) by intraperitoneal route with 7-day intervals among injections. Anesthetized mice were challenged intranasally for 3 consecutive days

with 30 µg of OVA Grade V (Sigma-Aldrich, St. Louis, MO, USA) 7 days after the third sensitization.

In vivo macrophage polarization during asthma

Mice were intranasally inoculated with 10^7 *Sp*-AC in 30 µL of PBS, as described above. For control, mice were inoculated with PBS alone by the same route. After 24 h, the animals were euthanized, and BALF was collected for cytokine detection. Cells in BALF were counted, lysed, and RNA was extracted for gene expression analysis by RT-qPCR.

Histology

The upper right lobes of the lungs were fixed in 4% formalin for 72 h, transferred to a solution of 70% ethanol and embedded in paraffin blocks. Sections were cut into 5 µm-thick sections and lungs were stained with hematoxylin and eosin (H&E).

Statistical analysis

Data were presented as the mean ± SEM and analyzed by Prism 8.0 (GraphPad Software, San Diego, CA). For comparisons between experimental groups, one-way ANOVA was performed followed by Bonferroni or Tukey's multiple comparisons post-tests. Individual groups were compared using the Student's *t*-test. Data that were not normally distributed were analyzed using the nonparametric Mann–Whitney test or Kruskal–Wallis test. Statistically significant differences were indicated by P values ≤ 0.05.

Supplementary Information The online version contains supplementary material available at https://doi.org/10.1007/s10495-023-01899-1.

Author contributions Conceived and designed the experiments: ACGS, LAP, AIM, VLDB, CHS. Performed the experiments: ACGS, LAP, LSP, BVB, KO, MB, GC. Analyzed the data: ACGS, LAP, NND, LSP, LR, AIM. Wrote the paper: LAP, NND, ACGS, AIM, VLDB, CHS. Provided Reagents: VLDB, CHS, AIM.

Funding This work was supported by São Paulo Research Foundation (FAPESP) and FAPESP fellowships (11/17611-7; 12/23580-0, 16/10964-5, 17/04786-0, 18/19638-9, 2020/09327-6, 2017/21629-5); the Brazilian National Council for Scientific and Technological Development – CNPq (471945/2012-9; 306363/2013-5; 307109/2016-0) and Coordenação de Aperfeiçoamento de Pessoal de Nível Superior - Brasil (CAPES) - Finance Code 001 and PROPG-UNESP/PROPE/UNESP.

Data availability The data that support the findings of this study are available from the corresponding author, Medeiros, AI, upon reasonable request.

Declarations

Competing interests The authors declare no competing interests.

Ethical approval All animal experiments were carried out under ethical guidelines and approved by the Institutional Animal Care and Committee from the School of Pharmaceutical Sciences, São Paulo State University—Number 59-2016, and from the School of Medicine, University of São Paulo—number 245/2019.

References

1. Doran AC, Yurdagul A Jr, Tabas I (2020) Efferocytosis in health and disease. Nat Rev Immunol 20:254–267. https://doi.org/10.1038/s41577-019-0240-6
2. Karaji N, Sattentau QJ (2017) Efferocytosis of pathogen-infected cells. Front Immunol 8:1863. https://doi.org/10.3389/fimmu.2017.01863
3. Penteado LDA, Dejani NN, Verdan FF, Orlando AB, Niño VE, Dias FDN, Salina ACG, Medeiros AI (2017) Distinctive role of efferocytosis in dendritic cell maturation and migration in sterile or infectious conditions. Immunology 151:304–313. https://doi.org/10.1111/imm.12731
4. Dejani NN, Orlando AB, Niño VE, Penteado LDA, Verdan FF, Bazzano JMR, Codo AC, Salina ACG, Saraiva AC, Avelar MR et al (2018) Intestinal host defense outcome is dictated by PGE2; production during efferocytosis of infected cells. Proc Natl Acad Sci USA 115:E8469. https://doi.org/10.1073/pnas.1722016115
5. Niño-Castaño VE, Penteado LdA, Silva-Pereira L, Bazzano JMR, Orlando AB, Salina ACG, Dejani NN, Bonato VLD, Serezani CH, Medeiros AI (2022) RIP2 contributes to expanded CD4+T cell IFN-γ production during efferocytosis of *Streptococcus pneumoniae*–infected apoptotic cells. ImmunoHorizons 6:559–568. https://doi.org/10.4049/immunohorizons.2200001
6. Torchinsky MB, Garaude J, Blander JM (2010) Infection and apoptosis as a combined inflammatory trigger. Curr Opin Immunol 22:55–62. https://doi.org/10.1016/j.coi.2010.01.003
7. Torchinsky MB, Garaude J, Martin AP, Blander JM (2009) Innate immune recognition of infected apoptotic cells directs TH17 cell differentiation. Nature 458:78–82. https://doi.org/10.1038/nature07781
8. Wculek SK, Heras-Murillo I, Mastrangelo A, Mañanes D, Galán M, Miguel V, Curtabbi A, Barbas C, Chandel NS, Enríquez JA et al (2023) Oxidative phosphorylation selectively orchestrates tissue macrophage homeostasis. Immunity 56:516-530.e519. https://doi.org/10.1016/j.immuni.2023.01.011
9. Watanabe S, Alexander M, Misharin AV, Budinger GRS (2019) The role of macrophages in the resolution of inflammation. J Clin Investig 129:2619–2628. https://doi.org/10.1172/JCI124615
10. Possa SS, Leick EA, Prado CM, Martins MA, Tibério IF (2013) Eosinophilic inflammation in allergic asthma. Front Pharmacol 4:46. https://doi.org/10.3389/fphar.2013.00046
11. Ray A, Kolls JK (2017) Neutrophilic inflammation in asthma and association with disease severity. Trends Immunol 38:942–954. https://doi.org/10.1016/j.it.2017.07.003
12. Moore WC, Hastie AT, Li X, Li H, Busse WW, Jarjour NN, Wenzel SE, Peters SP, Meyers DA, Bleecker ER (2014) Sputum neutrophil counts are associated with more severe asthma phenotypes using cluster analysis. J Allergy Clin Immunol 133:1557-1563.e1555. https://doi.org/10.1016/j.jaci.2013.10.011
13. Green RH, Brightling CE, Woltmann G, Parker D, Wardlaw AJ, Pavord ID (2002) Analysis of induced sputum in adults with asthma: identification of subgroup with isolated sputum neutrophilia and poor response to inhaled corticosteroids. Thorax 57:875–879. https://doi.org/10.1136/thorax.57.10.875
14. Talbot TR, Hartert TV, Mitchel E, Halasa NB, Arbogast PG, Poehling KA, Schaffner W, Craig AS, Griffin MR (2005) Asthma

as a risk factor for invasive pneumococcal disease. N Engl J Med 352:2082–2090. https://doi.org/10.1056/NEJMoa044113
15. Medeiros AI, Serezani CH, Lee SP, Peters-Golden M (2009) Efferocytosis impairs pulmonary macrophage and lung antibacterial function via PGE2/EP2 signaling. J Exp Med 206:61–68. https://doi.org/10.1084/jem.20082058
16. Reis AC, Alessandri AL, Athayde RM, Perez DA, Vago JP, Ávila TV, Ferreira TPT, de Arantes AC, de Sá Coutinho D, Rachid MA (2015) Induction of eosinophil apoptosis by hydrogen peroxide promotes the resolution of allergic inflammation. Cell Death Dis. 6:e1632–e1632. https://doi.org/10.1038/cddis.2014.580
17. Codo AC, Saraiva AC, dos Santos LL, Visconde MF, Gales AC, Zamboni DS, Medeiros AI (2018) Inhibition of inflammasome activation by a clinical strain of Klebsiella pneumoniae impairs efferocytosis and leads to bacterial dissemination. Cell Death Dis 9:1182. https://doi.org/10.1038/s41419-018-1214-5
18. Li Y, Li G, Zhang L, Li Y, Zhao Z (2022) G9a promotes inflammation in *Streptococcus pneumoniae* induced pneumonia mice by stimulating M1 macrophage polarization and H3K9me2 methylation in FOXP1 promoter region. Ann Transl Med. https://doi.org/10.21037/atm-22-1884
19. Dumigan A, Cappa O, Morris B, Sá Pessoa J, Calderon-Gonzalez R, Mills G, Lancaster R, Simpson D, Kissenpfennig A, Bengoechea JA (2022) In vivo single-cell transcriptomics reveal Klebsiella pneumoniae skews lung macrophages to promote infection. EMBO Mol Med 14:e16888. https://doi.org/10.15252/emmm.202216888
20. Gerlach BD, Ampomah PB, Yurdagul A, Liu C, Lauring MC, Wang X, Kasikara C, Kong N, Shi J, Tao W et al (2021) Efferocytosis induces macrophage proliferation to help resolve tissue injury. Cell Metabol 33:2445-2463.e2448. https://doi.org/10.1016/j.cmet.2021.10.015
21. Zysk G, Bejo L, Schneider-Wald BK, Nau R, Heinz H (2000) Induction of necrosis and apoptosis of neutrophil granulocytes by Streptococcus pneumoniae. Clin Exp Immunol 122:61–66. https://doi.org/10.1046/j.1365-2249.2000.01336.x
22. Häcker G (2018) Apoptosis in infection. Microbes Infect 20:552–559. https://doi.org/10.1016/j.micinf.2017.10.006
23. Koppe U, Suttorp N, Opitz B (2012) Recognition of *Streptococcus pneumoniae* by the innate immune system. Cell Microbiol 14(4):460–466
24. Goldmann O, von Köckritz-Blickwede M, Höltje C, Chhatwal GS, Geffers R, Medina E (2007) Transcriptome analysis of murine macrophages in response to infection with *Streptococcus pyogenes* reveals an unusual activation program. Infect Immun 75:4148–4157. https://doi.org/10.1128/iai.00181-07
25. Zhong X, Lee HN, Kim SH, Park SA, Kim W, Cha YN, Surh YJ (2018) Myc-nick promotes efferocytosis through M2 macrophage polarization during resolution of inflammation. FASEB J 32:5312–5325. https://doi.org/10.1096/fj.201800223R
26. Fadok VA, Bratton DL, Konowal A, Freed PW, Westcott JY, Henson PM (1998) Macrophages that have ingested apoptotic cells in vitro inhibit proinflammatory cytokine production through autocrine/paracrine mechanisms involving TGF-beta, PGE2, and PAF. J Clin Investig 101:890–898. https://doi.org/10.1172/jci1112
27. Guimarães-Pinto K, Maia EP, Ferreira JRM, Filardy AA (2022) Efferocytosis in lung mucosae: implications for health and disease. Immunol Lett 248:109–118. https://doi.org/10.1016/j.imlet.2022.07.005
28. Huynh ML, Fadok VA, Henson PM (2002) Phosphatidylserine-dependent ingestion of apoptotic cells promotes TGF-beta1 secretion and the resolution of inflammation. J Clin Investig 109:41–50. https://doi.org/10.1172/jci11638
29. Martinez J, Cook DN (2021) What is the deal with efferocytosis and asthma? Trends Immunol 42:904–919. https://doi.org/10.1016/j.it.2021.08.004
30. Fraga-Silva TFDC, Boko MMM, Martins NS, Cetlin AA, Russo M, Vianna EO, Bonato VLD (2023) Asthma-associated bacterial infections: are they protective or deleterious? J Allergy Clin Immunol: Global 2:14–22. https://doi.org/10.1016/j.jacig.2022.08.003
31. van der Veen TA, de Groot LES, Melgert BN (2020) The different faces of the macrophage in asthma. Curr Opin Pulm Med 26:62–68. https://doi.org/10.1097/mcp.0000000000000647
32. Li L, Cheng Y, Tu X, Yang J, Wang C, Zhang M, Lu Z (2020) Association between asthma and invasive pneumococcal disease risk: a systematic review and meta-analysis. Allergy Asthma Clin Immunol: Off J Can Soc Allergy Clin Immunol. https://doi.org/10.1186/s13223-020-00492-4
33. Hartmann C, Behrendt A-K, Henken S, Wölbeling F, Maus UA, Hansen G (2015) Pneumococcal pneumonia suppresses allergy development but preserves respiratory tolerance in mice. Immunol Lett 164:44–52. https://doi.org/10.1016/j.imlet.2014.12.001
34. Yang B, Liu R, Yang T, Jiang X, Zhang L, Wang L, Wang Q, Luo Z, Liu E, Fu Z (2015) Neonatal *Streptococcus pneumoniae* infection may aggravate adulthood allergic airways disease in association with IL-17A. PLoS ONE 10:e0123010. https://doi.org/10.1371/journal.pone.0123010
35. Martins NS, de Campos Fraga-Silva TF, Correa GF, Boko MMM, Ramalho LNZ, Rodrigues DM, Hori JI, Costa DL, Bastos JK, Bonato VLD, Artepillin C (2021) Reduces allergic airway inflammation by induction of monocytic myeloid-derived suppressor cells. Pharmaceutics 13:1763. https://doi.org/10.3390/pharmaceutics13111763